6572–6588 *Nucleic Acids Research, 2017, Vol. 45, No. 11* *Published online 24 May 2017*
doi: 10.1093/nar/gkx441

Krüppel-like factors compete for promoters and enhancers to fine-tune transcription

Melissa D. Ilsley[1,2], Kevin R. Gillinder[1], Graham W. Magor[1], Stephen Huang[1,2], Timothy L. Bailey[3], Merlin Crossley[4] and Andrew C. Perkins[1,2,5,*]

[1]Mater Research Institute, Translational Research Institute, University of Queensland, Brisbane 4102, Australia, [2]School of Biomedical Sciences, University of Queensland, Brisbane 4072, Australia, [3]Center for Molecular Medicine, University of Nevada, Reno, NV, USA, [4]University of New South Wales, Sydney 1466, Australia and [5]The Princess Alexandra Hospital, Brisbane 4102, Australia

Received April 19, 2017; Editorial Decision May 03, 2017; Accepted May 22, 2017

ABSTRACT

Krüppel-like factors (KLFs) are a family of 17 transcription factors characterized by a conserved DNA-binding domain of three zinc fingers and a variable N-terminal domain responsible for recruiting cofactors. KLFs have diverse functions in stem cell biology, embryo patterning, and tissue homoeostasis. KLF1 and related family members function as transcriptional activators via recruitment of co-activators such as EP300, whereas KLF3 and related members act as transcriptional repressors via recruitment of C-terminal Binding Proteins. KLF1 directly activates the *Klf3* gene via an erythroid-specific promoter. Herein, we show KLF1 and KLF3 bind common as well as unique sites within the erythroid cell genome by ChIP-seq. We show KLF3 can displace KLF1 from key erythroid gene promoters and enhancers *in vivo*. Using 4sU RNA labelling and RNA-seq, we show this competition results in reciprocal transcriptional outputs for >50 important genes. Furthermore, *Klf3*$^{-/-}$ mice displayed exaggerated recovery from anemic stress and persistent cell cycling consistent with a role for KLF3 in dampening KLF1-driven proliferation. We suggest this study provides a paradigm for how KLFs work in incoherent feed-forward loops or networks to fine-tune transcription and thereby control diverse biological processes such as cell proliferation.

INTRODUCTION

Krüppel-like factors are a group of 17 transcription factors (TFs) which play diverse roles in cell proliferation, differentiation and development (1). All 17 members contain highly conserved DNA-binding domains consisting of three C-terminal C_2H_2-type zinc fingers (2) which confer binding to a nine base pair CACCC-box DNA sequence, CCM–CRC–CCN, found in many tissue-specific gene promoters and enhancers (3). The Specificity Protein (SP) family of proteins are related to the KLFs (4) and bind similar motifs *in vivo* (5). SP/KLF proteins can be grouped into clades according to their N-terminal domains (Supplementary Figure S1A) (6). Krüppel-like factor 1 (KLF1), KLF2 and KLF4 primarily activate target genes by recruiting cofactors such as EP300 and CBP (7), whereas KLF3, KLF8 and KLF12 repress target genes by recruiting cofactors such as C-terminal binding proteins (CtBP1, CtBP2) (8–10). Other members of the SP/KLF family can repress or activate target genes depending on genomic context.

Multiple KLFs are often expressed in the same cells. In these situations, they can form transcriptional networks to coordinate developmental programs. For example, KLF2, KLF4 and KLF5 work redundantly in embryonic stem (ES) cells where they co-regulate key pluripotency genes such as *Nanog,* as well as each other, to maintain a 'stem cell-like' state (11). Many KLFs are expressed during erythropoiesis. These include *Klf1*, *Klf2*, *Klf3*, *Klf6* and *Klf10* (12). *Klf1*, the founding member of the KLF family (13), is erythroid-specific and is essential for definitive erythropoiesis (14,15). In fact, KLF1 controls nearly all aspects of erythropoiesis including globin gene regulation, haem biosynthesis and the cell cycle (3,16–20). Expression of *Klf3* is ubiquitous but is highest in erythroid tissue, the gut, skin, lungs, and the spleen (21). In erythroid cells, KLF1 directly activates *Klf3* via an erythroid-specific promoter as well as the ubiquitous promoter (22). Due to extensive homology in the DNA-binding domains (Supplementary Figure S1B), it is no surprise KLF1 and KLF3 bind to the same DNA motif *in vitro* (21,23). Furthermore, the preferred *in vivo* binding motif for KLF1 in erythroid cells and KLF3 in MEFs is identical (3,24). This presents the possibility that opposing biochemical functions of KLF1 and KLF3 may converge on the same transcriptional targets in the same cell type. Thus, we hypothesized KLF1 and KLF3 might compete for pro-

*To whom correspondence should be addressed. Tel: +61 73443 7573; Email: andrew.perkins@mater.uq.edu.au

moters and enhancers in erythroid cells resulting in 'fine-tuning' of gene regulation and cell proliferation and/or differentiation.

To address this hypothesis, we developed tamoxifen-inducible ER™ fusions of KLF1 and KLF3. We stably introduced these into erythroid cell lines to facilitate measurement of the direct transcriptional consequences of an induced DNA-binding event for each of the TFs. Following induction, we performed ChIP-seq and next-generation sequencing of newly synthesized RNA (4sU-RNA-seq), a metabolic labeling approach to qauntify recently transcribed RNA, including primary nuclear RNA, genome wide. This facilitates measurement of the immediate transcriptome consequences of a TF DNA-binding event (25). Using ChIP-seq, we show that KLF1 and KLF3 co-occupy promoters and enhancers of many critical erythroid genes such as *E2f2*. Furthermore, KLF3 can displace KLF1 from these sites. We identified a set of 54 genes inversely regulated by KLF1 and KLF3. Together, these data suggest that KLF3 acts to 'fine-tune' transcription in erythropoiesis by repressing genes activated by KLF1 and thereby dampening the KLF1-induced transcriptional response. This result is consistent with an incoherent type 1 feed-forward loop (FFL) or network (26,27), which we suggest is necessary for precise control over the tempo of erythrocyte proliferation. We validated this in $Klf3^{-/-}$ mice, which have near normal steady state erythropoiesis (28) but display increased sensitivity and an exaggerated rebound in response to phenylhydrazine-induced hemolysis. This study provides a paradigm for how the KLF/SP superfamily of TFs modulates gene expression to fine-tune biological responses in various cell systems.

MATERIALS AND METHODS

Generation of cell lines

K1-ER cells, previously known as B1.6 cells, were generated from $Klf1^{-/-}$ fetal liver-derived erythroid cells as previously described (29). The KLF3 ORF was cloned in frame with ERα into MSCV-IRES-GFP. The plasmid was transfected into GP+E86 cells (30) to generate a stable retrovirus-producing subclone. J2E cells were infected by co-culture with GP+E-Klf3-ER and sorted for GFP by FACS. Expression of the transgene was confirmed by western blotting using a mouse monoclonal antibody raised against ERα (Santa Cruz Biotechnology, HC-20, #sc-543).

Chromatin immunoprecipitation and sequencing (ChIP-seq)

K1-ER and J2E-Klf3-ER cell lines were incubated in 2 mM 4OH-tam (or ethanol vehicle control) for 3 h prior to crosslinking with 0.4% formaldehyde. KLF1-ER ChIP was performed with a rabbit polyclonal antibody raised against the N-terminus of KLF1 (15). Two replicates of KLF1-ER ChIP from two independent clones were combined for deeper analysis; one replicate was previously published (25). KLF3-ER ChIP was performed on a single clone selected for equivalent expression levels to K1-ER cells using a mouse monoclonal antibody against ERα (ThermoScientific, ss-315-P). Enrichment of specific target sites within ChIPed DNA was validated by qPCR (see additional methods). Samples ($n = 3$) were pooled to enhance complexity, used to generate Ion Xpress™ Plus fragment libraries and sequenced on the Ion Proton platform. Reads were mapped to the mouse genome (mm9) using TMAP, a best platform for Ion Torrent data (25,31); duplicate reads and multi-mapped reads were excluded. Peaks were called using MACS2 (32) and annotated with respect the peak position relative to the nearest gene; i.e. promoter, intron, UTR, CDS, downstream, distal and intergenic. Promoter regions were defined as –1 kb upstream and +75 bp downstream of the TSS. Downstream regions were defined as –75 bp upstream and +1 kb downstream of the TTS. Distal regions were defined as within 50 kb upstream or downstream of a gene. ChIP was validated by qPCR with reference to input DNA using primers (Supporting Table S1) designed to amplify DNA spanning the center of peaks and 1 kb up or downstream of the peaks.

Motif analysis of ChIP-seq data

De novo motif discovery was undertaken on peaks ±50 bp of DNA or ±250 bp of DNA using MEME with or without repeat masking (33). The results using ±50 bp of DNA and repeat masking were the most robust and are reported herein. To determine any preferential binding partners for KLF1 versus KLF3, MEME was run in discriminative mode. *De novo* matrices were compared with defined motifs as deposited in the JASPAR and UniProbe repositories using TOMTOM from MEME SUITE (36). Differential enrichment of short un-gapped motifs between KLF1 and KLF3 peaks (±50 bp) was also undertaken on peaks using Discriminative Regular Expression Motif Elicitation (DREME) (34). Over representation of defined DNA motifs as catalogued in JASPAR and UniProbe databases was performed using CentriMo within the MEME Suite (35).

We downloaded GATA1 ChIP-seq data in induced G1-ER4 cell line (GEO accession: GSM995443) (36). TAL1 ChIP-seq in MEL cell line (GEO accession number: GSM923578) (37). NFE2 ChIP-seq in Ter119+ sorted, phenylhydrazine-treated mice spleens (GEO accession number: GSM1151147) (38). FLI-1 ChIP-seq in mature megakaryocytes from murine E14.5 fetal liver (GEO accession: GSM1032607) (39).

4sU-RNA isolation and sequencing (4sU-RNA-seq)

4sU-RNA-seq was performed as previously described (25). Three clonally independent lines of J2E and J2E-KLF3-ER (clones A, C and E) cells were incubated with 2 mM 4OH-tam (or ethanol control) for 10 min prior to addition of 500 μM 4sU (Sigma; #T4509) then incubated for further 30 min. Enrichment for primary transcripts relative to spliced RNA was validated by qRT-PCR (see Supporting Table S2 for primers). 4sU-labeled RNA was used to generate Ion Xpress™ Plus fragment libraries which were sequenced on the Ion Proton platform. Reads were mapped to the mouse genome (mm9) using Tophat2 (40) and TMAP (31). Significantly differentially regulated genes (DEGs) were determined using CuffDiff (41) using a Bonferroni-corrected *q*-value cut-off of 0.05.

Collection of ChIP-seq tracks

ChIP-seq and DNase1-seq data from MEL cells were used for comparison with our generated data. Data sets were obtained from the Encyclopaedia of DNA Elements (ENCODE) project and visualised on the UCSC Genome Browser (42). Data sets used are GATA1 ChIP-seq in MEL cells (ENCFF001NSG), SCL/TAL1 ChIP-seq in MEL cells (ENCFF001MWV), p300 ChIP-seq in MEL cells (ENCFF001NXL), DNase1-seq in MEL cells (ENCFF001OOB), and H3K4me3 ChIP-seq in MEL cells (ENCFF001MZR). We compared read densities between ChIP-seq data sets using EaSeq (43).

CAGE data

CAGE data (44) was extracted from the Zenbu Genome Browser (45) FANTOM5 mouse time course study (46). The Phase2 pooled data from the J2E differentiation time course in response to EPO was accessed. CAGE tags over regions of the *Klf1* promoter and *Klf3* 1a and 1b promoters (22), corresponding the bars in Figure 1A, were exported from Zenbu as an XL file. CAGE is directional, so tags orientated in either direction were independently counted and graphed. Counts are reported as tags per million base pairs (TPM). Error bars represent the ± SEM of three biological replicates.

Luciferase reporter assays

Luciferase reporter assays were performed as previously described (20). Cloning of pPAC-Klf1 and pPAC-Klf3 has been previously described (21,47). pGL2-E2f2-for and pGL2-E2f2-rev reporter vectors have been previously described (20). Plasmids were transfected into Drosophila SL2 cells using Insectogene (Biontex) according to the manufacturer's instructions. Lysates were prepared and assayed for luciferase activity using the Dual-Luciferase Reporter Assay System (Promega, E1910) and fluorescence was quantified on a PHERAstar *FS* (BMG Labtech). Reported results are from $n = 4$ independent replicates per enhancer. Statistical significance was determined by one-way ANOVA. Error bars show standard deviation.

Analysis of stress erythropoiesis in *Klf3* knockout mice

Klf3 knockout mice (48) had been previously backcrossed onto a pure FVB/NJ genetic background. 8–12-week-old $Klf3^{-/-}$ mice and litter mates were injected with phenylhydrazine-HCl (PHZ) (Sigma #114715) at 60 mg/kg in PBS i.p. on day 0, as previously described (49). Blood (∼20 μl) was collected from the peri-orbital venous plexus into heparinised capillary tubes before PHZ (day 0) and again on days +2, +4 and +7. A complete blood count (CBC) was undertaken using a mindray BC-500 Vet AutoHaematology Analyser (Shenzhen, China). Mice were injected with 1 mg of BrdU (10 mg/ml stock) i.p. 90 min prior to sacrifice. Spleens were dispersed into single cells and stained with B220-PacBlue (BioLegend), CD3-PerCP/Cy5.5 (BioLegend), CD71-PE (BD Pharmingen), TER119-PE/Cy7 (BD Pharmingen) and Live/Dead Aqua (Life Technologies L34957) according to the manufacturer's recommendations. 10^6 spleen cells were fixed, permeabilized and stained with an FITC-conjugated antibody to BrdU and 7AAD according to BD Pharmingen kit #559619. FACS analysis of surface markers and cell cycle was performed on a BD LSRFortessa X-20. Cell sorting was performed using a BD FACSAria Fusion. Analysis and generation of plots was performed in FlowJo version 10.0.8. CD71+TER119+ cells were sorted into TRIzol (Thermo Fisher Scientific), total RNA was prepared according to the manufacturer's recommendations and cDNA was made using Superscript-III. qRT-PCR was performed using SyberGreen and specific intron-jumping primers listed in Supporting Table S3. Expression normalised to *Hprt* using delta CT method.

Software

Statistics analysis was performed with GraphPad Prism version 6.04 for Windows, GraphPad Software, La Jolla California USA, www.graphpad.com. Evolutionary tree of Krüppel-like factors and ClustalW alignment of KLF1/KLF3 were performed using the program Geneious version R7 (50). Hierarchical clustering and read density plots were generated using EaSeq (43), available from http://easeq.net/. Proportional Venn diagrams were generated with use of EulerAPE (51).

GEO accession numbers

The new ChIP-seq and RNA-seq data from this publication have been submitted to the Gene Expression Omnibus (GEO) and assigned the identifier GSE92620.

RESULTS

KLF3 occupies erythroid gene promoters and enhancers *in vivo*

We have recently performed ChIP-seq studies for KLF1 (25) in the murine J2E-like erythroid cell line, K1-ER (52). In order to generate a comparable dataset for KLF3, we ectopically expressed a tamoxifen-inducible version of KLF3 (KLF3-ER™) in J2E cells. The use of a tamoxifen-inducible fusion to KLF3 had two advantages. Firstly, the ER™ moiety acts as an epitope tag allowing ChIP. This is essential since no ChIP-grade KLF3 antibody is currently known. Secondly, fusion to the ligand-binding domain of ERα allows us to induce KLF3 activity via the addition of tamoxifen and observe dynamic effects on gene expression.

J2E cells were immortalised from wild type E14.5 murine fetal liver using the J2 retrovirus which expresses v-*raf* and v-*myc*. $Klf1^{-/-}$ J2E-like cells, K1-ER, were similarly generated previously using $Klf1^{-/-}$ E14.5 fetal liver and the same virus and conditions (29). J2E cells express *Klf1* and differentiate into mature erythroid cells in response to erythropoietin (53). Like primary erythroid cells, J2E cells markedly upregulate endogenous *Klf3* gene expression upon terminal differentiation as shown by high temporal resolution CAGE data (54) (Figure 1A). We generated clonally independent cells lines, dubbed J2E-Klf3-ER, in which 4-hydroxytamoxifen (4OH-tam)-induced nuclear levels of

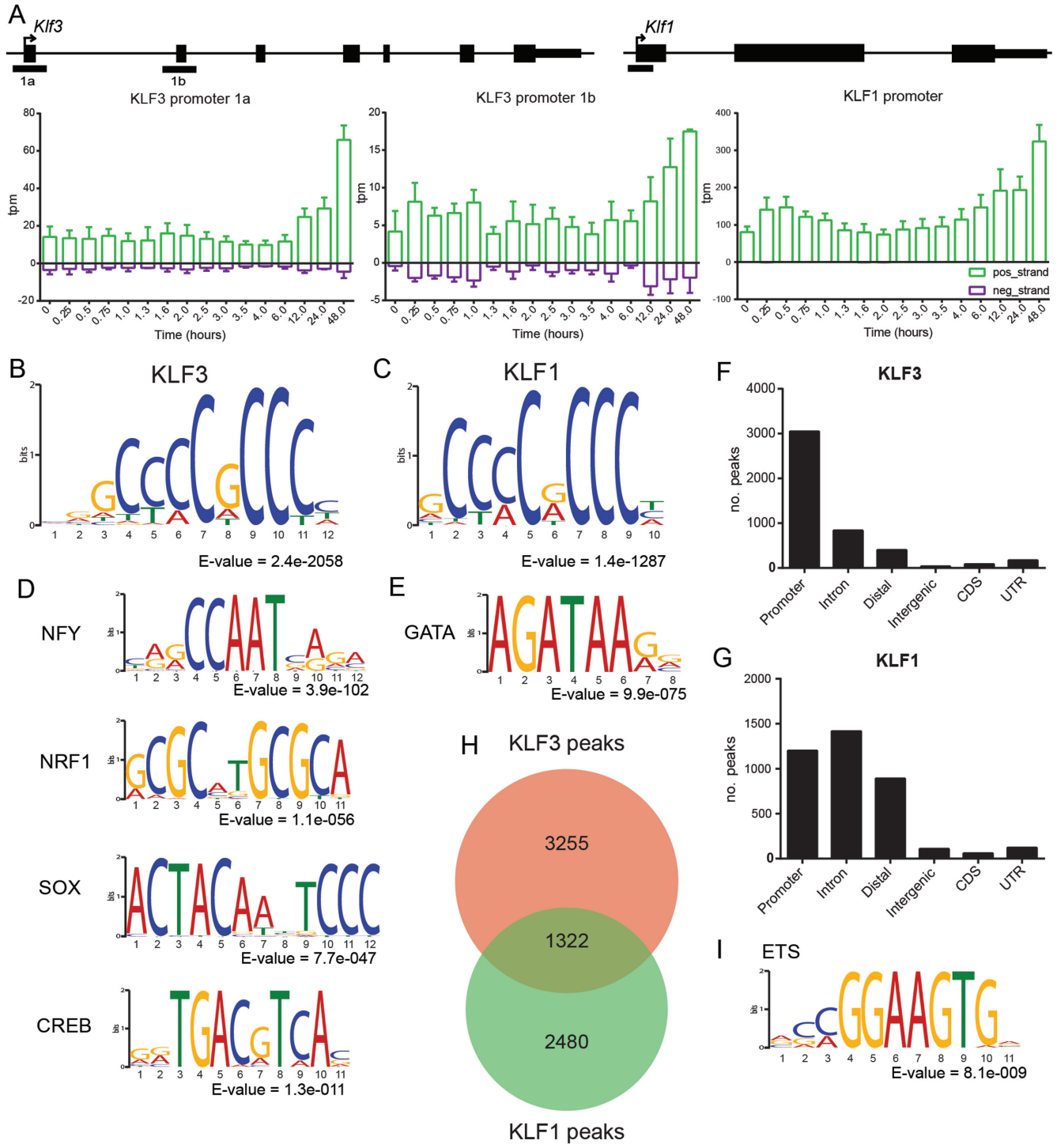

Figure 1. Overlapping and unique *in vivo* KLF3 and KLF1 binding characteristics. (**A**) CAGE tag density at the indicated regions (bars) of the *Klf3* 1a and 1b promoters and the *Klf1* promoter. Green bars indicate sense strand tags and purple bars antisense strand tags. Data were generated from the Zenbu web Browser. There is an increase in expression of KLF3 and KLF1 over a 48-h window of differentiation of J2E cells in response to EPO. (B, C) *De novo* motif binding specificity defined by MEME analysis performed on ±50 bp window around all peaks declared in KLF3-ER ChIP-seq data (**B**) and in KLF1-ER ChIP-seq data (**C**). (D, E) Position weighted matrices of secondary motifs identified using MEME on ±50 bp window around all peaks declared in KLF3-ER ChIP-seq data (**D**) and in KLF1-ER ChIP-seq data (**E**). (F, G) Distribution of ChIP-seq peak locations relative to genic landmarks for KLF3 ChIP-seq (**F**) and KLF1 ChIP-seq (**G**). (**H**) Venn diagram of overlap of KLF1 and KLF3 peaks as determined by MACS2. (**I**) ETS-like motif identified from discriminative MEME analysis.

KLF3 are 3–5-fold greater than endogenous KLF3. Thus, these new cell lines have comparable levels of nuclear KLF3 protein to the levels of nuclear KLF1 protein in K1-ER cells after addition of 4OH-tam (Supplementary Figure S2A) (25).

ChIP for KLF3 was performed at three hours post-induction with 4OH-tam, to be consistent with ChIP-seq for KLF1 in K1-ER cell lines (25). A total of 4579 peaks met a stringent threshold for peak-calling using MACS2 (32) (Supporting Table S4). *De novo* motif discovery using MEME (see Materials and Methods) identified a typical 9bp extended 'CACCC-box' motif (CCM–CRC–CCN) as the most significantly enriched motif (E-value = 2.4×10^{-2058}) and most frequent motif (3761/4579 = 82%) within DNA ±50 bp from the center of the KLF3 peaks (Figure 1B). The motif is identical to that preferred by an epitope tagged KLF3 in MEFs (24), and by KLF1 in K1-ER cells (25) and primary fetal liver erythroid cells (3). In fact, the motif is identical to the one bound *in vivo* by all other KLFs and SP family proteins studied to date (3,5,55–59). This is not surprising given the similarity of the DNA-binding domains of all family members (2) (Supplementary Figure S1).

To compare KLF3 binding with KLF1 binding, we used previously published ChIP-seq for KLF1 in K1-ER cells (25) with an additional replicate to improve statistical power. We detected a total of 3612 significant KLF1-occupied peaks (Supporting Table S5). As for KLF3, *de novo* motif discovery using MEME found a typical CACCC-box motif as the most highly significantly enriched (E-value = 1.4×10^{-1287}) and most abundant (2009/3612) motif in the KLF1-enriched DNA (Figure 1C). Local motif enrichment analysis using CentriMo (60) confirms central enrichment of CACCC-box motifs in both the KLF3 and KLF1 ChIP-seq data, validating the specificity of the ChIP (Supplementary Figure S3).

Peaks were classified into one of five groups based on location relative to genic regions (see Materials and Methods); i.e. promoter, intron, distal, intergenic, coding sequence (CDS) and untranslated region (UTR). KLF3 binds more often to promoters than elsewhere in the genome (Figure 1F), which is consistent with the findings of previous KLF3 ChIP-seq performed in MEFs (24). In contrast, KLF1 binds more frequently at intronic and distal regions, with only ∼30% of peaks found at promoters (Figure 1G), as previously reported for both primary fetal liver and immortalized erythroid cells (3,25).

KLF3 and KLF1 occupy common and unique promoters and enhancers

To assess the overlap between KLF3 and KLF1-occupied sites in erythroid cells, we defined co-occupancy as peak summits being within ±100 bp of each other. One third of all KLF3 peaks (1322/4553) were declared as 'shared' with KLF1 by these criteria (Figure 1H). MACS2 requires a significant read density relative to the background to pass a peak calling threshold (32), potentially leading to an under-representation of shared occupancy. To address this, we plotted read density over a region of ±10 kb from the summits of the union of peaks called in either KLF3 or KLF1 ChIP-seq data sets (total 7057 peaks) (see Materials and Methods) (Figure 2A). This representation of the data suggests greater overlap between KLF1-bound and KLF3-bound sites than is apparent from the Venn diagram in Figure 1H. In fact, most of the sites in the union are bound to some degree by both TFs. Nevertheless, there was a clear gradient of relative occupancy; i.e. the KLF1:KLF3 tag ratio and *vice versa* using hierarchical clustering within Easeq (43).

Although due to the limited resolution of ChIP-seq these data do not definitively establish that KLF1 and KLF3 bind to exactly the same sequence, a single 9 bp CCM–CRC–CCN consensus motif can be identified within the ChIPed DNA in many cases. Thus, given that peaks for both KLF1 and KLF3 are observed, the most likely explanation is that in these instances both KLF1 and KLF3 do bind the same site. Sites primarily bound predominantly by KLF3 show an even greater enrichment for promoters (Figure 2C). Conversely, sites primarily bound by KLF1 are enriched at intronic or distal regions as expected for enhancers (Figure 2E). Shared peaks show enrichment for promoters (Figure 2D).

KLF1 and KLF3 prefer the company of different transcription factors

It was not surprising to find KLF1 and KLF3 bind the same extended CACCC box motifs *in vivo* given the sequence identity of the DNA-binding residues (Supplementary Figure S1). So, something else must explain relative preference for different genomic locations. To investigate this, we first searched for additional *de novo* motifs in each of the ChIP-seq datasets using MEME (see Materials and Methods). The second most enriched motif in the KLF3-ChIPed DNA was CCAAT (Figure 1D), which is known to be bound by the tripartite, NFY A, B and C proteins (61–63). CCAAT boxes occurred in 239 of 4579 (5%) of all KLF3-occupied sites with an E-value of 3.9×10^{-102}. We also found statistically significant enrichment of an NRF1-like motif (179 sites; $E = 1.1 \times 10^{-56}$), a SOX-like motif (49 sites; $E = 7.7 \times 10^{-47}$) and a CREB-like motif (79 sites, $E = 1.3 \times 10^{-11}$) (Figure 1D). We used Tomtom to find the best matches to the *de novo* motifs within databases of deposited known motifs (see Materials and Methods). The SOX-like motif is an imperfect match to numerous SOX motifs, so it is difficult to be certain which TF it binds in erythroid cells (Supplementary Figure S4A). The NRF1-like motif is a good match to the NRF1 TFBS (Supplementary Figure S4B). The CREB-like motif could be bound by any one or more bZIP TF family member such as FOS/JUN, or the important erythroid and megakaryocyte transcription factor MafG(p18)/NF-E2(p45) heterodimer (Supplementary Figure S4C).

The second most enriched motif in the KLF1-ChIPed DNA was AGATAA, the preferred binding motif for GATA1 (Figure 1E). This is consistent with previous reports of co-operative *in vivo* binding of GATA1 and KLF1 (3). The GATA motif occurred in 203 of the peaks (6%) with an E-value of 9.9×10^{-75}. The only other statistically enriched motif was a GC-rich motif which differs from the CACCC-box at one nucleotide (Supplementary Figure S4D). This occurred 550 times with E-value of 3.0×10^{-10}. From analysis of known motifs using Tomtom it is

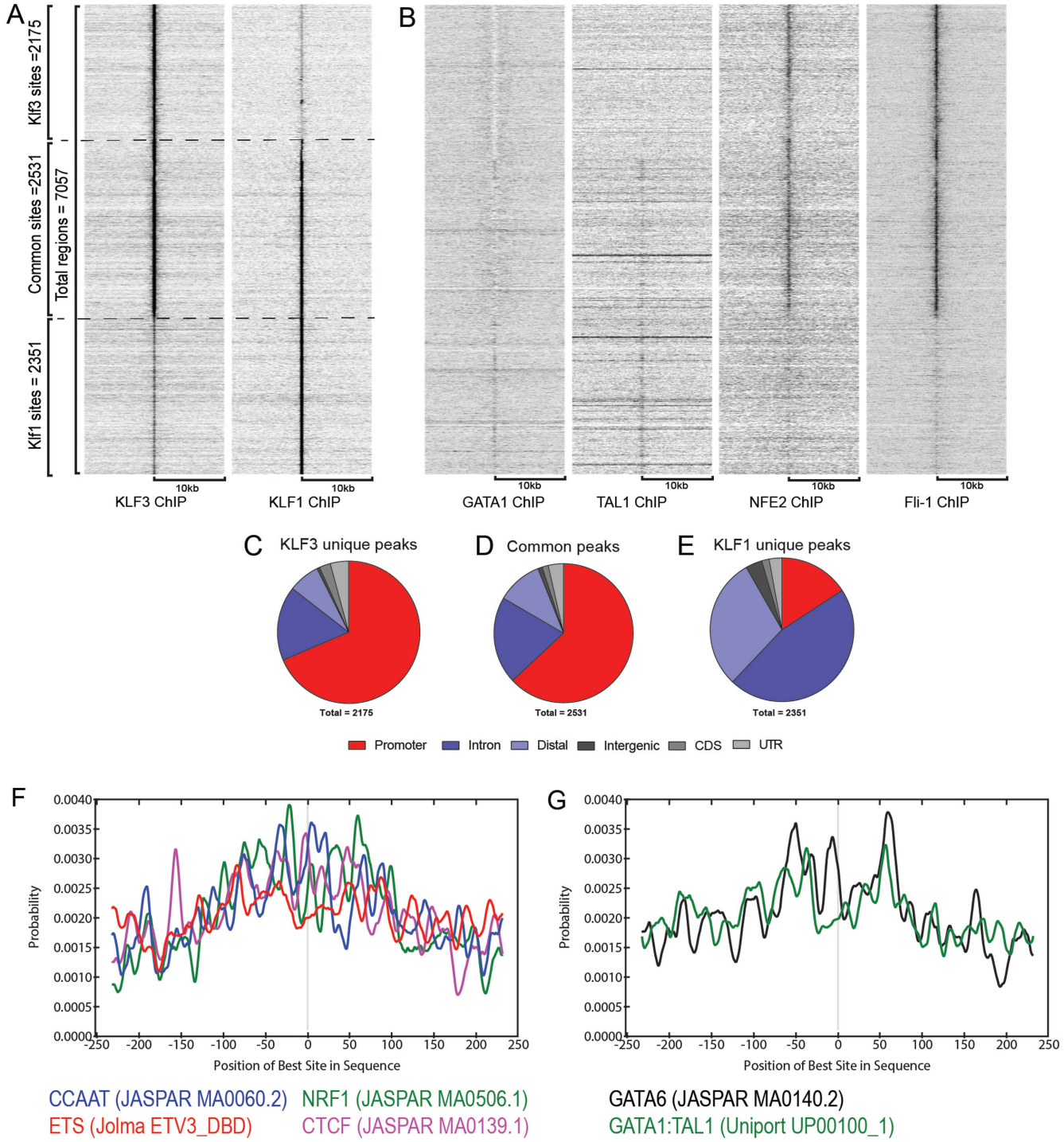

Figure 2. KLF1 and KLF3 bind unique and common genomic sites in erythroid cells. (**A**) Heat plot representation of ChIP-seq data. Rows represent genomic location around the summits of all peaks called in the union of both data sets, merged if summits are within 100 bp of each other. The left column represents KLF3 ChIP-seq reqad density and the center column represents KLF1 ChIP-seq read density. Regions were sorted according to hierarchical clustering using the nearest neighbour chain algorithm (95,96). Clustering was based on both ChIP-seq data sets using values quantified in an area ranging from –50 bp to +50 bp from the start of the regions. Plots were generated using EaSeq (43). (**B**) Heat plots of transcription factor ChIP-seq tag reads from erythroid and megakaryocytic cells compared with KLF1 and KLF3 ChIP–seq reads; GATA1 ChIP in G1ER cells, TAL1 ChIP-seq in MEL cells, NFE2 ChIP in TER119+ sorted erythrocytes and FLI-1 ChIP in sorted megakaryocytes (see Materials and Methods). (**C–E**) Pie charts displaying the distribution of peak summit regions from KLF1 and KLF3 ChIP-seq data separated by whether the region is significantly bound by KLF3-only (B), both KLF1 and KLF3 (C), or KLF1-only (D). (**F**) Analysis of motifs enriched in KLF3 ChIP peaks versus KLF1 ChIP peaks using CentriMo (see Materials and Methods). Centrally enriched motifs are provided below the graph. (**G**) Motifs enriched in KLF1 ChIP peaks versus KLF3 ChIP peaks as determined by CentriMo. Centrally enriched motifs are provided below the graph.

not clear what binds this motif. It may simply be a variant CACCC box. There were no other statistically significant motifs identified.

We also ran MEME in a discriminative mode whereby the combined KLF1 and KLF3 ChIPed DNA (peak summits ±50bp) was used to generate a background DNA sequence model and either the KLF1 or KLF3-occupied DNA (peak summits ±50bp) was analysed in reference to this model. The purpose was to enhance our ability to find specific motifs enriched in one versus the other datasets; i.e. what else influenced selective binding preferences (See Methods). We found the same motif enrichment in the DNA surrounding the KLF3 peaks using this approach as the non-discriminative approach, but we also identified an ETS-like motif (*E*-value = 8.1×10^{-9}) (Figure 1I). The ETS motif could be bound by FLI-1, ERG or some other ETS family TF (see Discussion). For the KLF1-occupied DNA we found no additional motifs. We also asked whether there were any novel short (6 bp) *de novo* motifs which could discriminate between the KLF3 'only' peaks (±50 bp from the summit; Supporting Table S5) and KLF1 'only' bound regions (±50 bp from the summit; Supporting Table S7) using DREME (see Materials and Methods). For KLF3, we found statistically significant over representation of a CREB motif (BGACGB; $E = 9.7 \times 10^{-37}$), a CCAAT box ($E = 5.8 \times 10^{-21}$), a partial NRF1-like motif (CAYGCG; $E = 6.7 \times 10^{-10}$), and a motif with similarities to partial GLI and ZBTB7A/LRF/Pokemon-binding sites (KGTCGS; $E = 2.3 \times 10^{-4}$) (Supplementary Figure S5A). For KLF1, we again found the GATA motif, WGATAW (*E* value = 2.3×10^{-68}) but nothing else of note (Supplementary Figure S5B).

As an alternative approach to find discriminative motifs between KLF1 'only' and KLF3 'only; bound DNA (groups defined in Figure 2A), we utilized CentriMo (Central Motif Enrichment Analysis). We asked whether known motifs from the combined JASPAR and UniProbe databases were relatively enriched in KLF3 versus KLF1-ChIPed DNA and *vice versa* (see Materials and Methods) (60). We found ETS motifs, such as for the ETV3 DBD (ACCGGAAGTg; *E*-value = 8.1×10^{-9}), were the most enriched in KLF3-occupied DNA (Figure 2H). We also confirmed over representation of NF-Y (CCAAT box; Fischer *E*-value = 3.1×10^{-7}), CREB-like (1.1×10^{-3}), NRF1 (1.3×10^{-2}), and weak over representation of CTCF TFBS (1.4×10^{-1}) in the KLF3-bound DNA (Figure 2F). There was an interesting offset of CCAAT boxes relative to the peak-central CACCC-box suggesting spacing might be important (Figure 2F). A similar spacing arrangement between CCAAT boxes and SP/KLF sites was recently reported in three different cell types for which there is extensive ENCODE ChIP-seq data (61). Interestingly, the KLF-related protein, SP2, also localises to promoters and is associated with NF-Y motifs in MEFs (5,62).

KLF1-only peaks were centrally enriched for GATA motifs (e.g. GATA6; Fisher *E*-value = 1.1×10^{-9}) (Figure 2G). These were also offset from the center consistent with spacing constraints between GATA and CACCC-box motifs. CentriMo found a TAL1:GATA1 combined motif with 8 bp spacing between the GATA and TAL1 half sites as previously reported (3) (Figure 2G). Using the CACCC-box as the primary motif we confirmed with full KLF1-GATA1-TAL1 combined motif using SpaMo (Supplementary Figure S5C).

Given these motif enrichments, we searched for evidence of actual co-binding of certain TFs with KLF1 or KLF3. We downloaded ChIP-seq data for GATA1 from G1-ER cells (a similar line to J2E), NF-E2 from primary erythroid cells, TAL1 from MEL cells, and FLI-1 from *in vitro* expanded megakaryocytes (Figure 2B). We found close overlap of KLF1, GATA1 and TAL1 TFBS suggesting co-operation between these three TFs at critical erythroid enhancers, as expected (3). This is consistent with models of how this TF complex regulates erythropoiesis. On the other hand, we found overlap between KLF3-occupied sites, NF-E2-occupied sites, and FLI-1 occupied sites (see Discussion). This is consistent with the motif discovery and enrichment analyses for KLF3. The sites co-occupied by KLF1 and KLF3 are bound by all of these TFs (Figure 2B), suggesting they are complex sites which might offer the opportunity for differential binding of erythroid and megakaryocytic TFs.

KLF3 and KLF1 inversely regulate a subset of genes in erythropoiesis

We have previously published microarray experiments which suggest KLF1 and KLF3 inversely regulate a subset of erythroid genes in the fetal liver (28,64). However, it can be difficult to distinguish direct target genes from indirect effects by transcriptome analyses in primary tissues with mixed cell populations and differentiation states. *Klf1*$^{-/-}$ fetal liver cells display severe defects in differentiation (15) and *Klf3* is expressed and functional in non-erythroid cells which might confound interpretation of these datasets (21). So, to identify changes in gene expression that are a direct consequence of KLF3 and/or KLF1 binding in erythroid cells, we utilized 4sU-RNA-seq (25). Importantly, this labeling approach, combined with tamoxifen-inducible expression, allows us to examine direct transcriptional consequences of an induced DNA-binding event in the context of native chromatin (25).

KLF3-regulated genes were identified by comparing the 4sU-enriched transcriptome of parental J2E ($n = 3$) versus J2E-KLF3-ER ($n = 3$) cell lines 1 h after KLF3-ER induction. 4sU-RNA enrichment was confirmed by qRT-PCR for primary transcripts and processed mRNA (Supplementary Figure S6A, B). A total of 182 genes were down-regulated, and 83 genes were up-regulated in response to KLF3 (Supporting Table S9). We used 4sU-RNA-seq data from 1 h of KLF1-ER induction in K1-ER cells (25) for comparison to the KLF3-dependant transcriptome. K1-ER cells have a similar baseline and KLF1-induced transcriptome to J2E cells (Spearmann correlation 0.85) as expected from the similar derivation approach (Supplementary Figure S6C). However, a total of 589 genes were upregulated, and 179 genes were down-regulated after induction of KLF1. By intersecting differentially expressed genes (DEGs) from both experiments, 54 genes were determined to be activated by KLF1 and repressed by KLF3 (Figure 3A and Supporting Table S10). Of these, many are known to be important erythroid genes found in previous studies as KLF1 target genes

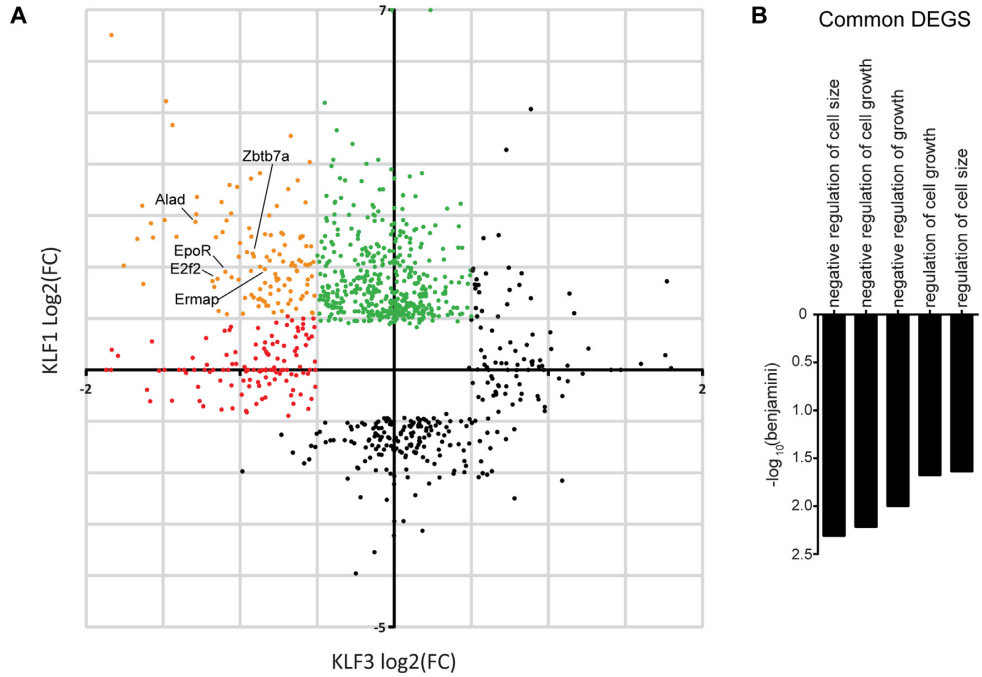

Figure 3. KLF1 and KLF3 inversely regulate many common genes *in vivo.* (**A**) Scatter plot of $\log_2$ (fold change) for genes differentially regulated by either KLF1 or KLF3; KLF1 Log_2(FC) on the y-axis and KLF3 $\log_2$(FC) on the x-axis. Red data points represent genes that are significantly down-regulated by Klf3 but not significantly regulated by KLF1. Green data points show genes that are significantly upregulated by Klf1 but not significantly regulated by KLF3. Yellow data points are genes significantly co-regulated. (**B**) Gene ontology of common differentially expressed genes (DEGs) using DAVID functional analysis tool.

(25,65). They encode proteins involved in heme biosynthesis (*Alad*) (65,66), cell cycle regulation (*E2f2*) (20), blood group antigens (*Ermap*/*Scianna*) (67) and other *Klfs* such as *Klf10* (28). Interestingly, Gene Ontogeny analysis of inversely regulated genes using the Database for Annotation, Visualization and Integrated Discovery (DAVID) v6.8 (68) shows enrichment for genes involved in positive or negative regulation of cell size and cell growth, but not for other aspects of terminal erythroid cell differentiation (Figure 3B).

Most inversely regulated genes are flanked by regions of KLF3 and KLF1 occupancy; i.e. within ±10 kb from the TSS. We plotted the normalized ChIP-seq read density for both KLF1 (green) and KLF3 (red) versus distance to the nearest TSS (Figure 4, which is derived from data in Supporting Table S10). In many cases, there is co-binding (yellow), but in some cases, there is also relatively specific binding of KLF1 or KLF3 (green and red domains, respectively) to different putative regulatory regions for the same target gene. For example, known KLF1 binding sites in the first introns of the *Alad* and *E2f2* genes are co-occupied by KLF3 (yellow; lines 10 and 17). Yet, the *Alad* promoter is only bound by KLF3 (red). Likewise, the downstream *E2f2* enhancer is only occupied by KLF1 (green). The inverse regulation of these genes is almost certainly a direct response of KLF1 and KLF3 binding to these proximal elements. It supports the observation that KLF1 and KLF3 may also compete for occupancy at many enhancers (shown in yellow; Figure 4).

KLF3 and KLF1 compete for regulatory elements

Visualization of the combined ChIP-seq and RNA-seq on the UCSC Browser as wiggle tracks was informative. For example, an intronic region just upstream of exon 2 in the *E2f2* gene is a validated KLF1-dependent enhancer (En2, Figure 5A) (20). KLF1 and KLF3 both bind this enhancer, as do erythroid transcription factors, GATA1 and TAL1, which work with KLF1 in certain contexts (3). The transcriptional co-activator, EP300, also binds this region which shows DNase1 hypersensitivity (Figure 5A). There is an additional KLF1/KLF3 co-occupied region in the middle of intron 1 (En1, Figure 5A) which binds EP300 but not GATA1 or SCL/TAL1. This region is likely to be a second KLF1/3-responsive, but GATA1 non-responsive, enhancer; this hypothesis remains untested.

To investigate if KLF1 and KLF3 can compete for occupancy at apparently shared binding regions, we performed ChIP for endogenous KLF1 in J2E-KLF3-ER cells before and after induction of KLF3-ER with 4OH-tam. At shared regions, such as the *E2f2* intronic enhancer and the *Ermap* promoter (Supplementary Figure S7), KLF1 occupancy was significantly reduced after induction of KLF3-ER (Figure 5B and C). However, at regions where only KLF1 binds, such as that found in the intron of *Phyhip*, binding was unaffected by KLF3 induction (Supplementary Figure S8A–C). No significant KLF1 enrichment was found at the KLF3-only bound region at the control *Nabp1* promoter as expected (Supplementary Figure S8B and D). In short, KLF3 displaces KLF1 from shared binding regions *in vivo*, so KLF1 and KLF3 directly compete for oc-

Figure 4. KLF1 and KLF3 bind shared and unique sites near the TSS of inversely regulated genes Heat map of the density of unique ChIP reads (minus input reads) for KLF1 (green) and KLF3 (red) ±20kb relative to the TSS of 54 co-regulated genes.

cupancy of key enhancers and promoters. Luciferase reporter assays confirm this competition for occupancy has functional consequences for transcriptional output. For example, the enhancer of *E2f2* (in either the forward and reverse orientation) is responsive to KLF1, as previously reported (20). Increasing amounts of KLF3 plasmid represses KLF1-driven activation in a dose-dependent fashion (Figure 5D and E). Together, these data suggest that KLF1 and KLF3 can compete for regulatory elements and supports our primary hypothesis that KLF3 and KLF1 inversely regulate common target genes via an incoherent FFL mechanism (27).

KLF1 and KLF3 can also inversely regulate genes through uniquely-bound regulatory elements

The majority of KLF1/KLF3 inversely regulated genes have promoters and enhancers bound by both factors (Figure 4). However, in some cases KLF1 and KLF3 can regulate the same gene from separate binding sites rather than a shared site. This is the case for the *Alad* gene, where KLF1 binds a known intronic enhancer (3,66) while KLF3 binds at both the promoter and the enhancer (Figure 4, line 10 and Figure 6A). ChIP-PCR at the promoter, enhancer, and sites up and downstream from both confirms competition between KLF1 and KLF3 at the enhancer only (Figure 6B). These examples suggest KLF3 can repress KLF1 target genes by competition for shared binding sites, particu-

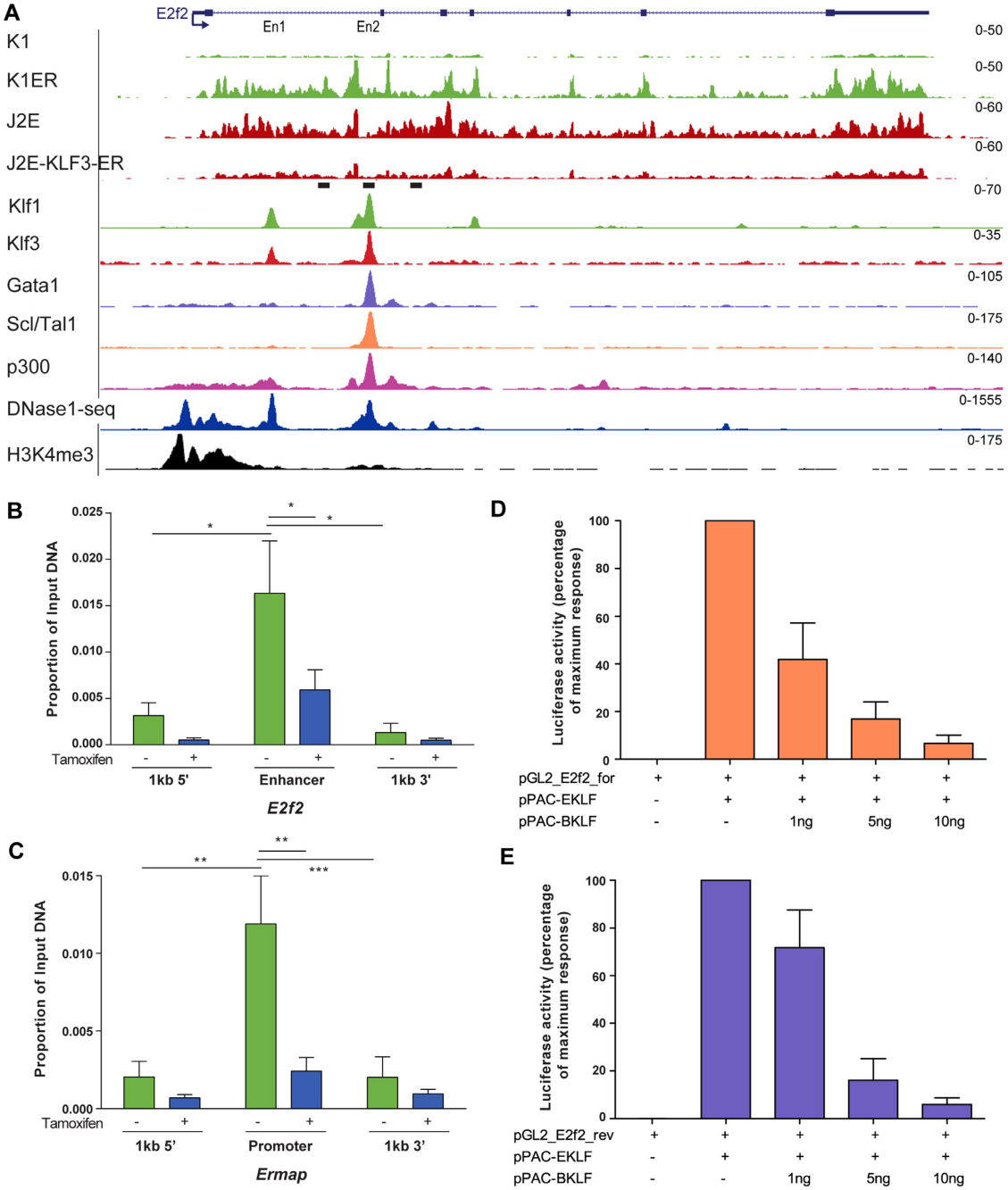

Figure 5. KLF1 and KLF3 binding leads directly to differential gene expression. (**A**) Image from the murine UCSC Genome Browser with read density graphs (wiggle plot) of a KLF1 and KLF3 common binding site at an intronic enhancer of *E2f2*. Top (red) track shows KLF1 ChIP-seq in K1-ER cells, second (green) track is KLF3 ChIP-seq in J2E-KLF3-ER cells, third (purple) track is GATA1 ChIP-seq data from MEL cells, fourth (orange) track is SCL/TAL1 ChIP-seq from MEL cells, fifth (pink) track shows EP300 ChIP-seq in MEL cells, sixth (blue) is a DNase-seq track in MEL cells, and seventh (black) track is H3K4me3 ChIP-seq from MEL cells. (B, C) ChIP-PCR of a KLF1 ChIP performed in J2E-KLF3-ER cells before (–) and after (+) induction with 4OH-tam at *E2f2* enhancer (**B**), and *Ermap* promoter (**C**). $*P > 0.05$, $**P > 0.005$, ns = not significant; by two-way ANOVA. Data are presented as mean ± SD ($n = 4$). (D, E) Luciferase reporter assays performed using the *E2f2* intronic enhancer in the forward (**D**) and reverse (**E**) orientations. Data are presented as mean ± SD ($n = 4$). $P = 0.0005$ (A); $P < 0.0001$ (B) by one-way ANOVA.

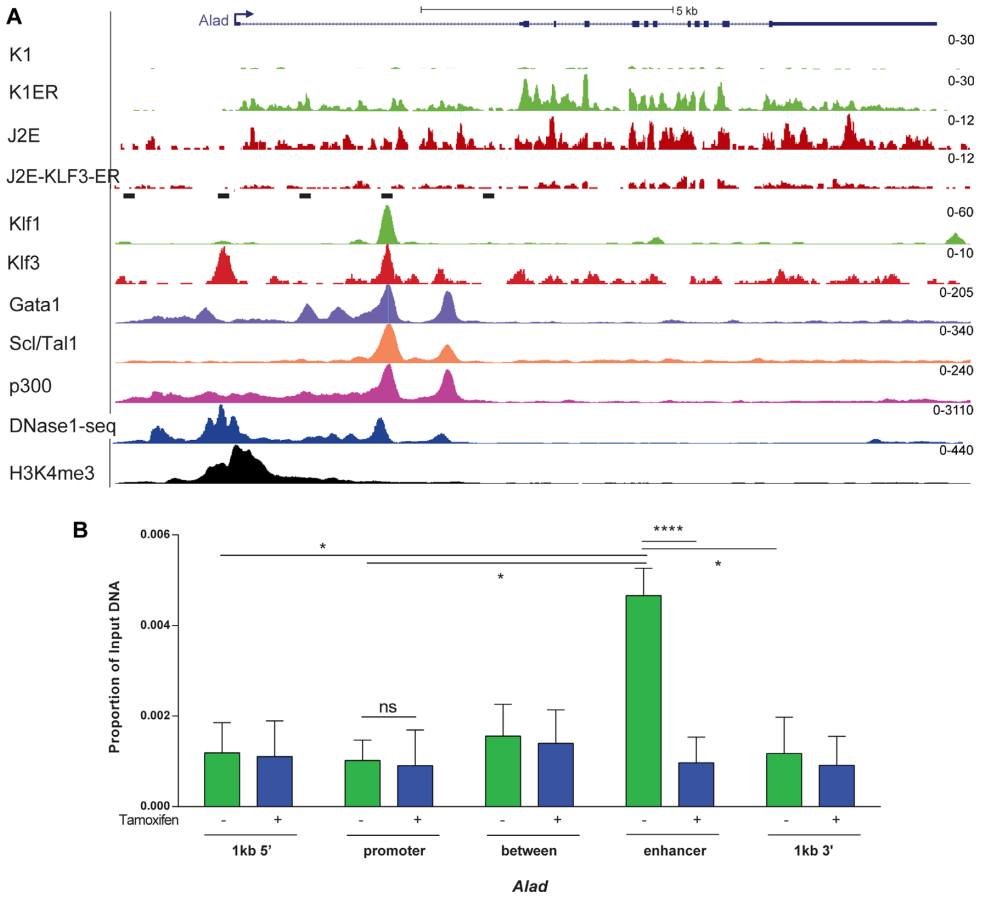

Figure 6. KLF1 and KLF3 can regulate genes through different binding sites. (**A**) UCSC Genome Browser wiggle plots at the *Alad* gene. Black bars represent region amplified by qPCR in section B. Figure details as per Figure 5A. (**B**) ChIP-PCR analysis of a KLF1 ChIP performed in J2E-KLF3-ER cells before and after induction of KLF3-ER with 4OH-tam at the *Alad* promoter, enhancer and flanking regions.

larly in enhancers, but also by directly binding to promoters which do not bind KLF1.

Klf3 null mice display increased sensitivity but exaggerated recovery from stress erythropoiesis and persistent cell cycling

We hypothesized that *Klf3*$^{-/-}$ mice would have an exaggerated response to hemolysis due to the lack of a negative feedback pathway required to inhibit the pro-proliferative activity of KLF1. To test this, we induced acute hemolytic stress in *Klf3*$^{-/-}$ mice and litter mate controls by i.p. injection of phenylhydrazine (60 mg/kg) (see Materials and Methods). We followed the CBC of mice for 7 days and discovered *Klf3*$^{-/-}$ mice develop more severe anemia at the nadir (day 3), but rebound more quickly than litter mates with a more pronounced reticulocytosis (Figure 7A and B) (see Materials and Methods). Furthermore, spleen cells from *Klf3*$^{-/-}$ mice have increased S phase in recovery compared with litter mates (Figure 7C), consistent with a failure to place a physiological break on DNA replication. This result was reproducible in additional litters, but varies somewhat in magnitude between experiments.

There is no overt block in differentiation in *Klf3*$^{-/-}$ erythroid cells as the percentage of CD71^{+}TER119^{+} and CD71^{-}TER119^{+} cells is equivalent in *Klf3*$^{-/-}$ mice and their litter mates (Supplementary Figure S9). Furthermore, the blood smears of recovering *Klf3*$^{-/-}$ mice are relatively normal apart from polychromasia due to reticulocytosis (data not shown). We sorted CD71^{+}TER119^{+} cells for analysis of gene expression by qRT-PCR. We also found only a moderate increase in *E2f2* expression in *Klf3*$^{-/-}$ fetal liver (Figure 7D) whereas expression is markedly reduced in *Klf1*$^{-/-}$ fetal liver (20). In fact, the overlap between KLF3-dependent DEGs in fetal liver (24) and the cell lines is not dramatic (Supplementary Figure S10), but there are many possible explanations for this. For example, (i) the cell lines represent just one cell type present in the fetal liver (i.e. the pro-erythroblast); (ii) there are additional cell types in fetal liver in which *Klf3* is expressed but *Klf1* is not (e.g. macrophages) and the signal from these cells will bias results and (iii) there is possible redundancy between other members of the KLF3 subclade of TFs *in vivo* that obscures the contribution of Klf3, but which is apparent in the short time frame captured by 4sU RNA-seq. Our results on the *Klf8* gene are relevant to this hypothesis. We find upregulation of *Klf8* in *Kf3*$^{-/-}$ primary erythroid cells (Figure 7E) as previously reported (28). Like KLF3, KLF8 functions predominantly as a transcriptional repressor via recruitment of CtBPs. *In vivo* redundancy between *Klf3* and *Klf8* is strongly suggested by the fact double knockout mice die early in de-

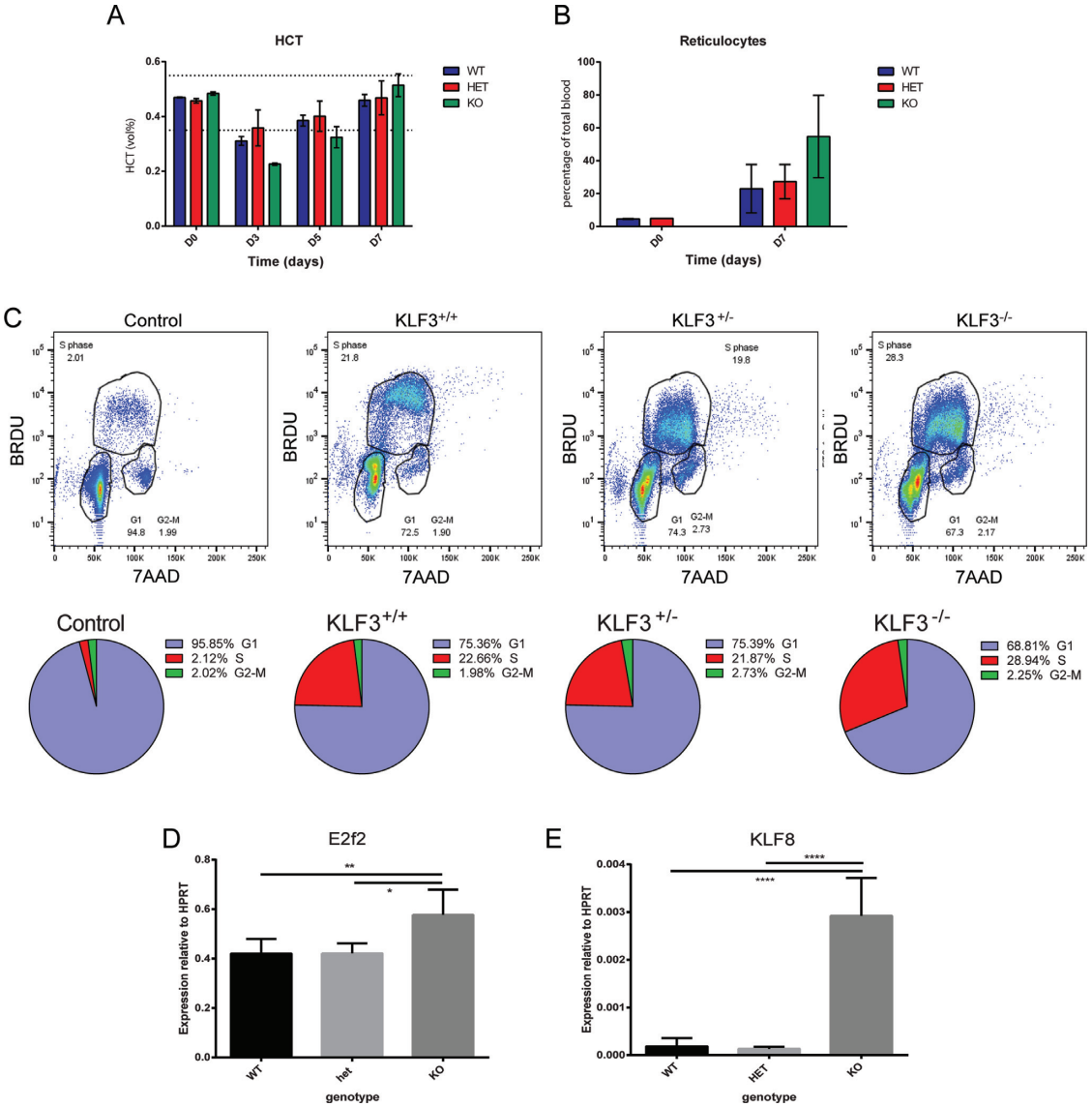

Figure 7. Klf3$^{-/-}$ mice display an exaggerated recovery and persistent cell cycling following phenylhydrazine treatment (**A** and **B**). Dynamic changes in hematocrit and reticulocytes following phenylhydrazine treatment of Klf3 wildtype, heterozygous and knockout mice over a 7-day period. (**C**) Cell cycle analyses of spleen cells harvested at D7 following phenylhydrazine treatment. For each genotype, we have plotted BrdU incorporation (DNA-synthesis) versus 7AAD labeling level (DNA content). (D and E) RT-PCR of E2f2 (**D**) and KLF8 (**E**) expression in fetal livers from 14.5dpc KLF3 mouse cross. Error bars display standard deviation from mean. * represent significant p-value (*$P > 0.05$, **$P > 0.005$, ****$P > 0.00005$)

velopment whereas single knockout mice for either TF are viable (69).

DISCUSSION

We have directly addressed whether two KLFs from different clades (KLF1 and KLF3) with opposing biochemical functions, can bind to the same enhancers and promoters in the same cell type (erythroid cells) to 'fine-tune' gene expression. Different KLFs are co-expressed in the many cell types often alongside SP family members. This this is the first study that directly addresses whether they can compete for the same promoters or enhancers *in vivo* and whether they can functionally antagonise each other.

Previous work has shown KLF1 is an important erythroid transcription factor that primarily binds enhancers and super-enhancers (3,70) to activate gene expression (Figure 6A). We recently found an extended repertoire of KLF1-occupied enhancers in erythroid cell lines (25), which are immortalized at the pro-erythroblast stage of differentiation. This is primarily due to technical advances resulting in greater sequencing depth and reduced background noise compared with previously published work (3). Many of these enhancers are not occupied by KLF3 (Figure 8A), so it is unclear whether other KLF/SP proteins can compete with KLF1 at these enhancers to limit the activity of KLF1. We found more than 4000 KLF3-occupied sites in the erythroid cell genome; these were primarily at promoters of non-expressed genes. Thus, KLF3 likely plays a role in

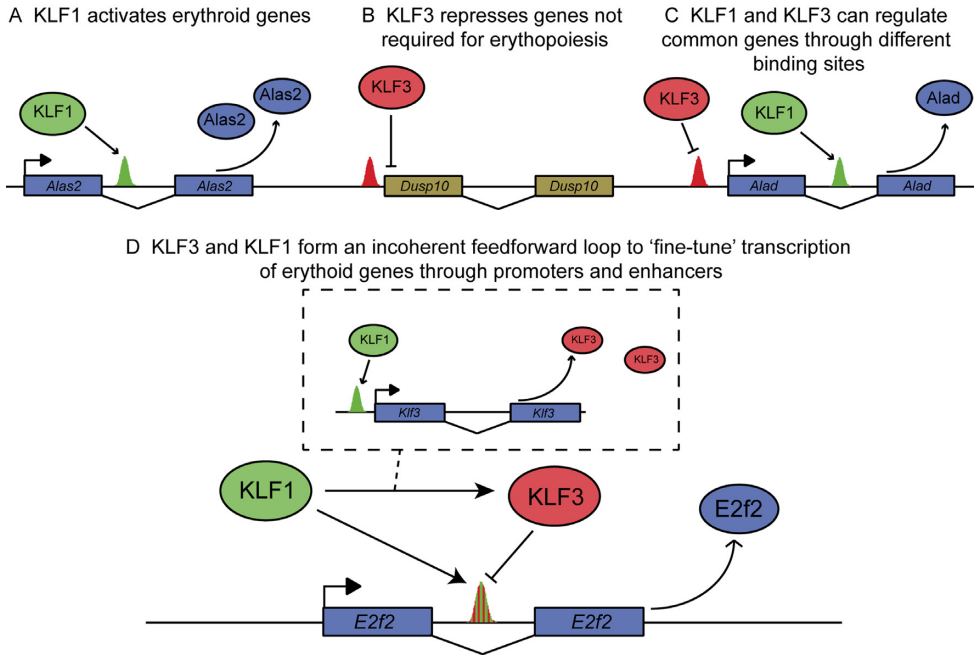

Figure 8. Model of transcriptional control by competition between KLF3 and KLF1. (**A**) Regulation of a KLF1 target genes independently of KLF3 feedback, leading to activation of gene expression. (**B**) Regulation of a KLF3 target gene which is independent of KLF1, leading to repression of gene expression. (**C**) KLF1 and KLF3 inversely regulate common genes from different locations. In this example, KLF3 binds to the promoter to reduce gene expression while KLF1 binds to an enhancer to increase gene expression. Overall, this leads to a fine-tuning of gene expression. (**D**) KLF1 and KLF3 bind to the same site in inversely regulated genes. Competition between the two transcription factors leads to fine-tuning of gene expression.

active repression of genes whose expression in not required (Figure 8B). This observation is consistent with our previous published work in MEFs (24). Some KLF3-occupied promoters had KLF1-occupied enhancers elsewhere in the same gene (e.g. *Alad*), suggesting KLF3 can also repress erythroid genes via a KLF1-independent mechanism (Figure 8C).

We found KLF3 preferentially binds promoters whereas KLF1 prefers enhancers, so we asked, 'why'? One possible answer resides in the non-DNA-binding domains of the proteins which recruit different co-activator and co-repressor proteins and may physically interact with other TFs. For example, KLF1 might be able to directly or indirectly interact with TAL1 and/or GATA1 and this interaction might be facilitated by the precise spacing of complimentary DNA-binding motifs in enhancers (3). Similarly, KLF3 might directly or indirectly interact with TFs to facilitate its preference for promoters. Using *de novo* motif discovery and statistical analyses of relative over representation of defined motifs, we found KLF3 prefers to bind in the neighborhood of CCAAT boxes, NRF1 motifs, ETS motifs, CREB motifs and to a lesser extent, CTCF and LRF/Pokemon motifs (Figures 1 and 2).

It is difficult to know whether KLF3 is recruited to promoters because of a physical interaction (direct or indirect) with NF-Y protein components and/or with NRF1 (which are both promoter-trophic TFs), or whether the motifs are simply enriched because KLF3 binds promoters for other reasons (71–73). There is an historical association between the CCAAT and CACCC (or GC-box) in basal gene promoters including those directing erythroid gene expression; e.g. both motifs are critical within the β-globin gene promoter (74). There is also extensive evidence of functional synergy between SP family proteins and NF-Y proteins using promoter-reporter assays (75), and for physical interactions between SP proteins and NF-Y components, particularly NF-YA (76). Also, there is recent published evidence that SP2 can bind DNA indirectly via interaction with NF-Y proteins (5). Further biochemical and mutational studies would be required to distinguish whether KLF3 (like SP factors) can physically interact with NF-Y components, facilitate or inhibit NF-Y promoter occupancy, and/or functionally antagonise NF-Y driven promoter activity. We have previously reported deletion of the N-terminal domain of KLF3 leads to specific failure to bind promoters in MEFs (24). This result might suggest direct or indirect physical interactions between the N-terminus of KLF3 and NF-Y components facilitates KLF3 promoter occupancy.

The enrichment of ETS motifs in KLF3-bound DNA suggests ETS-domain proteins such as FLI-1, ERG and PU.1 might bind near to KLF3. ETS proteins are important for megakaryopoiesis, hematopoietic stem cell function, myelopoiesis and lymphopoiesis. Indeed, we find FLI-1-bound sites in megakaryocytes and KLF3-bound sites in pro-erythroblasts overlap (Figure 2). Our ChIP-seq data does not necessarily argue KLF3 binds alongside FLI-1 in pro-erythroblasts. Rather, KLF3 and ETS proteins could bind the same genomic regions in different cell types or compete for binding in bi-potent progenitor cells (MEPs). Interestingly, over expression of KLF1 can suppress *Fli1* and the megakaryocytic program (77,78), whereas loss of KLF1 results in lineage infidelity and upregulation

of megakaryocytic genes such as *Itga2b* (which encoded CD41) and *Pf4* in erythroid cells (79). Lastly, conditional knockout of *Fli1* leads to erythroid hyperplasia (80). We suggest some of these effects might be mediated via KLF3 which is itself a direct KLF1-target gene (22). For example, binding of KLF3 to FLI-1-occupied sites might repress the megakaryocytic program in erythroid cells. Likewise, KLF3 binding to PU.1-occupied regions might suppress myelopoeisis. In this way, KLF3 could influence lineage decisions via antagonism of lineage specific ETS-binding proteins.

We found a subset of KLF1-bound regions that are co-bound by KLF3. Most of these are important erythroid enhancers such as the *E2f2* intron 1 enhancers (Figure 8D). We used 4sU metabolic labeling of new transcripts and RNA-seq to show reciprocal regulation of 54 genes (including *E2f2*) after induced overexpression of KLF1 or KLF3. This suggests an important incoherent type 1 FFL (27) in which KLF3 can 'fine tune' erythroid gene expression driven by KLF1 (Figure 8D). We confirmed dose-dependent reciprocal regulation of *E2f2* using enhancer-reporter assays, and modest upregulation of *E2f2* in *Klf3*$^{-/-}$ fetal liver and adult spleen. Interestingly, we found an exaggerated proliferation state and enhanced S phase on *Klf3*$^{-/-}$ splenic erythroid cells following recovery from hemolytic stress (Figure 7). Together, these results suggest KLF3 provides a physiological brake on KLF1-induced proliferation through competition for critical enhancers.

Of the 54 inversely regulated genes, three encode SERTAD (SERTA Domain Containing) genes. SERTADs have been shown to enhance the transcriptional activity of the E2F family of TFs (81,82). Both *E2f2* and *E2f4* have known roles in erythropoiesis (83,84). So, it is possible the SERTAD proteins are playing an important role in the regulation of DNA replication during erythroid development via their ability to modulate the function of E2F proteins. Interestingly, it has been recently reported that KLF10 regulates *Sertad1* in pancreatic tissue (85). SERTADs might regulate the function of additional TFs to the E2Fs. Thus, KLF1 and KLF3 could also indirectly 'fine-tune' the function of many TFs by inversely regulating the production of the co-activating SERTAD proteins.

Three *Klf* genes are themselves reciprocal targets of KLF1 and KLF3 in erythroid cells; i.e. *Klf10* (*Tieg*), *Klf11* (*Tieg2*) and *Klf16* (Figure 4). KLF1 and KLF3 both bind the *Klf11* gene promoters which are reciprocally regulated. Additionally, KLF1 activates *Klf9* and *Klf13* independently of KLF3, while KLF3 represses *Klf6*. *Klf11* gene knockout mice exhibit a mild erythroid phenotype (86). Other KLFs have not been studied in detail in an erythroid cell context although previous work suggests many are expressed (12). So, there are likely to be additional KLF networks at play during erythroid cell differentiation, and these might further tune gene expression.

KLF networks are important in many other cell types. For example *Klf2*, *Klf3* and *Klf4* are co-expressed in myeloid cells. Conditional gene knockouts of *Klf4* and *Klf2* indicated they are important for proper myeloid cell differentiation and function, respectively (87,88). An early report suggests *Klf3* knockout mice produce an excess of white blood cells (89), but this has not been investigated in detail. KLF2, KLF4 and KLF5 bind to each other's promoters as well as to critical stem cell gene promoters and enhancers in ES cells to provide a coherent FFL (27) which underpins the ES cell transcriptional state, or 'stemness' state (11,90). Could members of the KLF3/8/12 clade compete for occupancy at key ES cell enhancers and the promoters to displace KLF2/4/5 and thereby facilitate ES cell differentiation via engagement of an incoherent FFL? Similarly, KLF4 (or Gut Krüppel-like factor) and KLF5 (or Intestinal Krüppel-like factor) are both expressed in the gut epithelium in overlapping patterns (91,92). We suggest KLF3, which is also highly expressed in the gut, could compete with activating KLFs to regulate the turnover of the gut epithelium. KLF4 and KLF3 are also both expressed in the skin. KLF4 gene knockout mice die within 24 hours of birth due to dehydration because and they display defective terminal differentiation and cornification of the skin (93). Interestingly, *Klf3* is a direct target of KLF4 in the skin (94). No skin defects have been described in *Klf3* knockout mice, but this is worth exploring.

In summary, our study demonstrates functional competition between KLF1 and KLF3 for enhancers and promoters in erythroid cells. This fine-tunes the transcriptional response of target genes. Since the *Klf3* gene is itself a direct target of KLF1, we suggest an incoherent KLF3 feedforward network is wired to provide a brake on the transcriptional activation by KLF1, and that this is important for cell proliferation. Since activating and repressing KLFs are co-expressed in most cell types, we suggest these studies provide a paradigm for how KLF feedforward networks can be tempered by the KLF3/8/12 clade of KLFs (Figure 8C).

ACCESSION NUMBERS

The new ChIP-seq and RNA-seq data from this publication have been submitted to the Gene Expression Omnibus (GEO) and assigned the identifier GSE92620.

SUPPLEMENTARY DATA

Supplementary Data are available at NAR Online.

ACKNOWLEDGEMENTS

We thank Philip Koh for the provision of the MSCV-Klf3-ER plasmid.
Author contributions: M.D.I. undertook most of the experiments, generated the figures and co-wrote the manuscript, K.R.G. undertook wet laboratory experiments and bioinformatic analyses and provided technical supervision to M.D.I., G.W.M. undertook bioinformatic analyses, S.H. assisted with ChIP and data analyses, M.P.C. contributed to the experimental plan and proof-read the manuscript, T.L.B. undertook bioinformatic analyses and proof-read the manuscript and A.C.P. contributed to experimental design and co-wrote the manuscript.

FUNDING

National Health and Medical Research Council (NHMRC) [APP1082439]. Funding for open access charge: NHMRC [APP1082439].

Conflict of interest statement. None declared.

REFERENCES

1. Kaczynski,J., Cook,T. and Urrutia,R. (2003) Sp1- and Kruppel-like transcription factors. *Genome Biol.*, **4**, 206.
2. van Vliet,J., Crofts,L.A., Quinlan,K.G., Czolij,R., Perkins,A.C. and Crossley,M. (2006) Human KLF17 is a new member of the Sp/KLF family of transcription factors. *Genomics*, **87**, 474–482.
3. Tallack,M.R., Whitington,T., Yuen,W.S., Wainwright,E.N., Keys,J.R., Gardiner,B.B., Nourbakhsh,E., Cloonan,N., Grimmond,S.M., Bailey,T.L. *et al.* (2010) A global role for KLF1 in erythropoiesis revealed by ChIP-seq in primary erythroid cells. *Genome Res.*, **20**, 1052–1063.
4. Suske,G., Bruford,E. and Philipsen,S. (2005) Mammalian SP/KLF transcription factors: bring in the family. *Genomics*, **85**, 551–556.
5. Volkel,S., Stielow,B., Finkernagel,F., Stiewe,T., Nist,A. and Suske,G. (2015) Zinc finger independent genome-wide binding of Sp2 potentiates recruitment of histone-fold protein Nf-y distinguishing it from Sp1 and Sp3. *PLoS Genet.*, **11**, e1005102.
6. Presnell,J.S., Schnitzler,C.E. and Browne,W.E. (2015) KLF/SP transcription factor family evolution: expansion, diversification, and innovation in eukaryotes. *Genome Biol. Evol.*, **7**, 2289–2309.
7. Zhang,W., Kadam,S., Emerson,B.M. and Bieker,J.J. (2001) Site-specific acetylation by p300 or CREB binding protein regulates erythroid Kruppel-like factor transcriptional activity via its interaction with the SWI-SNF complex. *Mol. Cell. Biol.*, **21**, 2413–2422.
8. Dewi,V., Kwok,A., Lee,S., Lee,M.M., Tan,Y.M., Nicholas,H.R., Isono,K., Wienert,B., Mak,K.S., Knights,A.J. *et al.* (2015) Phosphorylation of Kruppel-like factor 3 (KLF3/BKLF) and C-terminal binding protein 2 (CtBP2) by homeodomain-interacting protein kinase 2 (HIPK2) modulates KLF3 DNA binding and activity. *J. Biol. Chem.*, **290**, 8591–8605.
9. van Vliet,J., Turner,J. and Crossley,M. (2000) Human Kruppel-like factor 8: a CACCC-box binding protein that associates with CtBP and represses transcription. *Nucleic Acids Res.*, **28**, 1955–1962.
10. Turner,J. and Crossley,M. (1998) Cloning and characterization of mCtBP2, a co-repressor that associates with basic Kruppel-like factor and other mammalian transcriptional regulators. *EMBO J.*, **17**, 5129–5140.
11. Jiang,J., Chan,Y.S., Loh,Y.H., Cai,J., Tong,G.Q., Lim,C.A., Robson,P., Zhong,S. and Ng,H.H. (2008) A core Klf circuitry regulates self-renewal of embryonic stem cells. *Nat. Cell Biol.*, **10**, 353–360.
12. Redmond,L.C., Dumur,C.I., Archer,K.J., Haar,J.L. and Lloyd,J.A. (2008) Identification of erythroid-enriched gene expression in the mouse embryonic yolk sac using microdissected cells. *Dev. Dyn.*, **237**, 436–446.
13. Miller,I.J. and Bieker,J.J. (1993) A novel, erythroid cell-specific murine transcription factor that binds to the CACCC element and is related to the kruppel family of nuclear proteins. *Mol. Cell. Biol.*, **13**, 2776–2786.
14. Nuez,B., Michalovich,D., Bygrave,A., Ploemacher,R. and Grosveld,F. (1995) Defective haematopoiesis in fetal liver resulting from inactivation of the EKLF gene. *Nature*, **375**, 316–318.
15. Perkins,A.C., Sharpe,A.H. and Orkin,S.H. (1995) Lethal B-thalassaemia in mice lacking the erythroid CACCC-transcription factor EKLF. *Nature*, **375**, 318–322.
16. Perkins,A., Xu,X., Higgs,D.R., Patrinos,G.P., Arnaud,L., Bieker,J.J., Philipsen,S. and Workgroup,K.L.F.C. (2016) Kruppeling erythropoiesis: an unexpected broad spectrum of human red blood cell disorders due to KLF1 variants. *Blood*, **127**, 1856–1862.
17. Magor,G.W., Tallack,M.R., Gillinder,K.R., Bell,C.C., McCallum,N., Williams,B. and Perkins,A.C. (2015) KLF1-null neonates display hydrops fetalis and a deranged erythroid transcriptome. *Blood*, **125**, 2405–2417.
18. Pilon,A.M., Arcasoy,M.O., Dressman,H.K., Vayda,S.E., Maksimova,Y.D., Sangerman,J.I., Gallagher,P.G. and Bodine,D.M. (2008) Failure of terminal erythroid differentiation in EKLF-deficient mice is associated with cell cycle perturbation and reduced expression of E2F2. *Mol. Cell. Biol.*, **28**, 7394–7401.
19. Gnanapragasam,M.N., McGrath,K.E., Catherman,S., Xue,L., Palis,J. and Bieker,J.J. (2016) EKLF/KLF1-regulated cell cycle exit is essential for erythroblast enucleation. *Blood*, **128**, 1631–1641.
20. Tallack,M.R., Keys,J.R., Humbert,P.O. and Perkins,A.C. (2009) EKLF/KLF1 controls cell cycle entry via direct regulation of E2f2. *J. Biol. Chem.*, **284**, 20966–20974.
21. Crossley,M., Whitelaw,E., Perkins,A., Williams,G., Fujiwara,Y. and Orkin,S.H. (1996) Isolation and characterization of the cDNA encoding BKLF/TEF-2, a major CACCC-box-binding protein in erythroid cells and selected other cells. *Mol. Cell. Biol.*, **16**, 1695–1705.
22. Funnell,A.P., Maloney,C.A., Thompson,L.J., Keys,J., Tallack,M., Perkins,A.C. and Crossley,M. (2007) Erythroid Kruppel-like factor directly activates the basic Kruppel-like factor gene in erythroid cells. *Mol. Cell. Biol.*, **27**, 2777–2790.
23. Perkins,A. (1999) Erythroid Kruppel like factor: from fishing expedition to gourmet meal. *Int. J. Biochem. Cell Biol.*, **31**, 1175–1192.
24. Burdach,J., Funnell,A.P., Mak,K.S., Artuz,C.M., Wienert,B., Lim,W.F., Tan,L.Y., Pearson,R.C. and Crossley,M. (2014) Regions outside the DNA-binding domain are critical for proper in vivo specificity of an archetypal zinc finger transcription factor. *Nucleic Acids Res.*, **42**, 276–289.
25. Gillinder,K.R., Ilsley,M.D., Nebor,D., Sachidanandam,R., Lajoie,M., Magor,G.W., Tallack,M.R., Bailey,T., Landsberg,M.J., Mackay,J.P. *et al.* (2017) Promiscuous DNA-binding of a mutant zinc finger protein corrupts the transcriptome and diminishes cell viability. *Nucleic Acids Res.*, **45**, 1130–1143.
26. Mangan,S., Itzkovitz,S., Zaslaver,A. and Alon,U. (2006) The incoherent feed-forward loop accelerates the response-time of the gal system of Escherichia coli. *J. Mol. Biol.*, **356**, 1073–1081.
27. Kim,D., Kwon,Y.K. and Cho,K.H. (2008) The biphasic behavior of incoherent feed-forward loops in biomolecular regulatory networks. *Bioessays*, **30**, 1204–1211.
28. Funnell,A.P., Norton,L.J., Mak,K.S., Burdach,J., Artuz,C.M., Twine,N.A., Wilkins,M.R., Power,C.A., Hung,T.T., Perdomo,J. *et al.* (2012) The CACCC-binding protein KLF3/BKLF represses a subset of KLF1/EKLF target genes and is required for proper erythroid maturation in vivo. *Mol. Cell. Biol.*, **32**, 3281–3292.
29. Coghill,E., Eccleston,S., Fox,V., Cerruti,L., Brown,C., Cunningham,J., Jane,S. and Perkins,A. (2001) Erythroid Kruppel-like factor (EKLF) coordinates erythroid cell proliferation and hemoglobinization in cell lines derived from EKLF null mice. *Blood*, **97**, 1861–1868.
30. Markowitz,D., Goff,S. and Bank,A. (1988) A safe packaging line for gene transfer: separating viral genes on two different plasmids. *J. Virol.*, **62**, 1120–1124.
31. Cartwright,D.A., Troggio,M., Velasco,R. and Gutin,A. (2007) Genetic mapping in the presence of genotyping errors. *Genetics*, **176**, 2521–2527.
32. Zhang,Y., Liu,T., Meyer,C.A., Eeckhoute,J., Johnson,D.S., Bernstein,B.E., Nusbaum,C., Myers,R.M., Brown,M., Li,W. *et al.* (2008) Model-based analysis of ChIP-Seq (MACS). *Genome Biol.*, **9**, R137.
33. Bailey,T.L., Williams,N., Misleh,C. and Li,W.W. (2006) MEME: discovering and analyzing DNA and protein sequence motifs. *Nucleic Acids Res.*, **34**, W369–W373.
34. Bailey,T.L. (2011) DREME: motif discovery in transcription factor ChIP-seq data. *Bioinformatics*, **27**, 1653–1659.
35. Bailey,T.L., Boden,M., Buske,F.A., Frith,M., Grant,C.E., Clementi,L., Ren,J., Li,W.W. and Noble,W.S. (2009) MEME SUITE: tools for motif discovery and searching. *Nucleic Acids Res.*, **37**, W202–W208.
36. Jain,D., Mishra,T., Giardine,B.M., Keller,C.A., Morrissey,C.S., Magargee,S., Dorman,C.M., Long,M., Weiss,M.J. and Hardison,R.C. (2015) Dynamics of GATA1 binding and expression response in a GATA1-induced erythroid differentiation system. *Genomics Data*, **4**, 1–7.
37. Pope,B.D., Ryba,T., Dileep,V., Yue,F., Wu,W., Denas,O., Vera,D.L., Wang,Y., Hansen,R.S., Canfield,T.K. *et al.* (2014) Topologically associating domains are stable units of replication-timing regulation. *Nature*, **515**, 402–405.
38. Hughes,J.R., Roberts,N., McGowan,S., Hay,D., Giannoulatou,E., Lynch,M., De Gobbi,M., Taylor,S., Gibbons,R. and Higgs,D.R.

(2014) Analysis of hundreds of cis-regulatory landscapes at high resolution in a single, high-throughput experiment. *Nat. Genet.*, **46**, 205–212.
39. Zang,C., Luyten,A., Chen,J., Liu,X.S. and Shivdasani,R.A. (2016) NF-E2, FLI1 and RUNX1 collaborate at areas of dynamic chromatin to activate transcription in mature mouse megakaryocytes. *Scientific Rep.*, **6**, 30255.
40. Trapnell,C., Williams,B.A., Pertea,G., Mortazavi,A., Kwan,G., van Baren,M.J., Salzberg,S.L., Wold,B.J. and Pachter,L. (2010) Transcript assembly and quantification by RNA-Seq reveals unannotated transcripts and isoform switching during cell differentiation. *Nat. Biotechnol.*, **28**, 511–515.
41. Trapnell,C., Roberts,A., Goff,L., Pertea,G., Kim,D., Kelley,D.R., Pimentel,H., Salzberg,S.L., Rinn,J.L. and Pachter,L. (2012) Differential gene and transcript expression analysis of RNA-seq experiments with TopHat and Cufflinks. *Nat. Protoc.*, **7**, 562–578.
42. Dunham,I., Kundaje,A., Aldred,S., Collins,P., Davis,C., Doyle,F., Epstein,C., Frietze,S., Harrow,J., Kaul,R. *et al.* (2012) An integrated encyclopedia of DNA elements in the human genome. *Nature*, **489**, 57–74.
43. Lerdrup,M., Johansen,J.V., Agrawal-Singh,S. and Hansen,K. (2016) An interactive environment for agile analysis and visualization of ChIP-sequencing data. *Nat. Struct. Mol. Biol.*, **23**, 349–357.
44. Arner,E., Daub,C.O., Vitting-Seerup,K., Andersson,R., Lilje,B., Drablos,F., Lennartsson,A., Ronnerblad,M., Hrydziuszko,O., Vitezic,M. *et al.* (2015) Transcribed enhancers lead waves of coordinated transcription in transitioning mammalian cells. *Science*, **347**, 1010–1014.
45. Severin,J., Lizio,M., Harshbarger,J., Kawaji,H., Daub,C.O., Hayashizaki,Y., Bertin,N. and Forrest,A.R. (2014) Interactive visualization and analysis of large-scale sequencing datasets using ZENBU. *Nat. Biotechnol.*, **32**, 217–219.
46. Lizio,M., Harshbarger,J., Abugessaisa,I., Noguchi,S., Kondo,A., Severin,J., Mungall,C., Arenillas,D., Mathelier,A., Medvedeva,Y.A. *et al.* (2016) Update of the FANTOM web resource: high resolution transcriptome of diverse cell types in mammals. *Nucleic Acids Res.*, **45**, D737–D743.
47. Merika,M. and Orkin,S.H. (1995) Functional synergy and physical interactions of the erythroid transcription factor GATA-1 with the Kruppel family proteins Sp1 and EKLF. *Mol. Cell. Biol.*, **15**, 2437–2447.
48. Sue,N., Jack,B.H., Eaton,S.A., Pearson,R.C., Funnell,A.P., Turner,J., Czolij,R., Denyer,G., Bao,S., Molero-Navajas,J.C. *et al.* (2008) Targeted disruption of the basic Kruppel-like factor gene (Klf3) reveals a role in adipogenesis. *Mol. Cell. Biol.*, **28**, 3967–3978.
49. Lee,H.Y., Gao,X., Barrasa,M.I., Li,H., Elmes,R.R., Peters,L.L. and Lodish,H.F. (2015) PPAR-alpha and glucocorticoid receptor synergize to promote erythroid progenitor self-renewal. *Nature*, **522**, 474–477.
50. Kearse,M., Moir,R., Wilson,A., Stones-Havas,S., Cheung,M., Sturrock,S., Buxton,S., Cooper,A., Markowitz,S., Duran,C. *et al.* (2012) Geneious Basic: an integrated and extendable desktop software platform for the organization and analysis of sequence data. *Bioinformatics*, **28**, 1647–1649.
51. Micallef,L. and Rodgers,P. (2014) eulerAPE: drawing area-proportional 3-Venn diagrams using ellipses. *PLoS ONE*, **9**, e101717.
52. Klinken,S.P., Nicola,N.A. and Johnson,G.R. (1988) In vitro-derived leukemic erythroid cell lines induced by a raf- and myc-containing retrovirus differentiate in response to erythropoietin. *Proc. Natl. Acad. Sci. U.S.A.*, **85**, 8506–8510.
53. Tilbrook,P.A., Colley,S.M., McCarthy,D.J., Marais,R. and Klinken,S.P. (2001) Erythropoietin-stimulated Raf-1 tyrosine phosphorylation is associated with the tyrosine kinase Lyn in J2E erythroleukemic cells. *Arch. Biochem. Biophys.*, **396**, 128–132.
54. Andersson,R., Gebhard,C., Miguel-Escalada,I., Hoof,I., Bornholdt,J., Boyd,M., Chen,Y., Zhao,X., Schmidl,C., Suzuki,T. *et al.* (2014) An atlas of active enhancers across human cell types and tissues. *Nature*, **507**, 455–461.
55. Terrados,G., Finkernagel,F., Stielow,B., Sadic,D., Neubert,J., Herdt,O., Krause,M., Scharfe,M., Jarek,M. and Suske,G. (2012) Genome-wide localization and expression profiling establish Sp2 as a sequence-specific transcription factor regulating vitally important genes. *Nucleic Acids Res.*, **40**, 7844–7857.
56. Aksoy,I., Giudice,V., Delahaye,E., Wianny,F., Aubry,M., Mure,M., Chen,J., Jauch,R., Bogu,G.K., Nolden,T. *et al.* (2014) Klf4 and Klf5 differentially inhibit mesoderm and endoderm differentiation in embryonic stem cells. *Nat. Commun.*, **5**, 3719.
57. Chen,X., Xu,H., Yuan,P., Fang,F., Huss,M., Vega,V.B., Wong,E., Orlov,Y.L., Zhang,W., Jiang,J. *et al.* (2008) Integration of external signaling pathways with the core transcriptional network in embryonic stem cells. *Cell*, **133**, 1106–1117.
58. Loft,A., Forss,I., Siersbaek,M.S., Schmidt,S.F., Larsen,A.S., Madsen,J.G., Pisani,D.F., Nielsen,R., Aagaard,M.M., Mathison,A. *et al.* (2015) Browning of human adipocytes requires KLF11 and reprogramming of PPARgamma superenhancers. *Genes Dev.*, **29**, 7–22.
59. Ying,M., Tilghman,J., Wei,Y., Guerrero-Cazares,H., Quinones-Hinojosa,A., Ji,H. and Laterra,J. (2014) Kruppel-like factor-9 (KLF9) inhibits glioblastoma stemness through global transcription repression and integrin alpha6 inhibition. *J. Biol. Chem.*, **289**, 32742–32756.
60. Bailey,T.L. and Machanick,P. (2012) Inferring direct DNA binding from ChIP-seq. *Nucleic Acids Res.*, **40**, e128.
61. Dolfini,D., Zambelli,F., Pedrazzoli,M., Mantovani,R. and Pavesi,G. (2016) A high definition look at the NF-Y regulome reveals genome-wide associations with selected transcription factors. *Nucleic Acids Res.*, **44**, 4684–4702.
62. Suske,G. (2016) NF-Y and SP transcription factors - New insights in a long-standing liaison. *Biochim. Biophys. Acta*, **1860**, 590–597.
63. Testa,A., Donati,G., Yan,P., Romani,F., Huang,T.H., Vigano,M.A. and Mantovani,R. (2005) Chromatin immunoprecipitation (ChIP) on chip experiments uncover a widespread distribution of NF-Y binding CCAAT sites outside of core promoters. *J. Biol. Chem.*, **280**, 13606–13615.
64. Hodge,D., Coghill,E., Keys,J., Maguire,T., Hartmann,B., McDowall,A., Weiss,M., Grimmond,S. and Perkins,A. (2006) A global role for EKLF in definitive and primitive erythropoiesis. *Blood*, **107**, 3359–3370.
65. Tallack,M.R., Magor,G.W., Dartigues,B., Sun,L., Huang,S., Fittock,J.M., Fry,S.V., Glazov,E.A., Bailey,T.L. and Perkins,A.C. (2012) Novel roles for KLF1 in erythropoiesis revealed by mRNA-seq. *Genome Res.*, **22**, 2385–2398.
66. Desgardin,A.D., Abramova,T., Rosanwo,T.O., Kartha,S., Shim,E.H., Jane,S.M. and Cunningham,J.M. (2012) Regulation of delta-aminolevulinic acid dehydratase by kruppel-like factor 1. *PLoS One*, **7**, e46482.
67. Ye,T.Z., Gordon,C.T., Lai,Y.H., Fujiwara,Y., Peters,L.L., Perkins,A.C. and Chui,D.H. (2000) Ermap, a gene coding for a novel erythroid specific adhesion/receptor membrane protein. *Gene*, **242**, 337–345.
68. Dennis,G. Jr., Sherman,B.T., Hosack,D.A., Yang,J., Gao,W., Lane,H.C. and Lempicki,R.A. (2003) DAVID: database for annotation, visualization, and integrated discovery. *Genome Biol.*, **4**, P3.
69. Funnell,A.P., Mak,K.S., Twine,N.A., Pelka,G.J., Norton,L.J., Radziewic,T., Power,M., Wilkins,M.R., Bell-Anderson,K.S., Fraser,S.T. *et al.* (2013) Generation of mice deficient in both KLF3/BKLF and KLF8 reveals a genetic interaction and a role for these factors in embryonic globin gene silencing. *Mol. Cell. Biol.*, **33**, 2976–2987.
70. Hay,D., Hughes,J.R., Babbs,C., Davies,J.O., Graham,B.J., Hanssen,L.L., Kassouf,M.T., Oudelaar,A.M., Sharpe,J.A., Suciu,M.C. *et al.* (2016) Genetic dissection of the alpha-globin super-enhancer in vivo. *Nat. Genet.*, **48**, 895–903.
71. Benner,C., Konovalov,S., Mackintosh,C., Hutt,K.R., Stunnenberg,R. and Garcia-Bassets,I. (2013) Decoding a signature-based model of transcription cofactor recruitment dictated by cardinal cis-regulatory elements in proximal promoter regions. *PLoS Genet.*, **9**, e1003906.
72. FitzGerald,P.C., Shlyakhtenko,A., Mir,A.A. and Vinson,C. (2004) Clustering of DNA sequences in human promoters. *Genome Res.*, **14**, 1562–1574.
73. Domcke,S., Bardet,A.F., Adrian Ginno,P., Hartl,D., Burger,L. and Schubeler,D. (2015) Competition between DNA methylation and transcription factors determines binding of NRF1. *Nature*, **528**, 575–579.

74. Myers,R.M., Tilly,K. and Maniatis,T. (1986) Fine structure genetic analysis of a beta-globin promoter. *Science*, **232**, 613–618.
75. Wright,K.L., Moore,T.L., Vilen,B.J., Brown,A.M. and Ting,J.P. (1995) Major histocompatibility complex class II-associated invariant chain gene expression is up-regulated by cooperative interactions of Sp1 and NF-Y. *J. Biol. Chem.*, **270**, 20978–20986.
76. Yamada,K., Tanaka,T., Miyamoto,K. and Noguchi,T. (2000) Sp family members and nuclear factor-Y cooperatively stimulate transcription from the rat pyruvate kinase M gene distal promoter region via their direct interactions. *J. Biol. Chem.*, **275**, 18129–18137.
77. Frontelo,P., Manwani,D., Galdass,M., Karsunky,H., Lohmann,F., Gallagher,P.G. and Bieker,J.J. (2007) Novel role for EKLF in megakaryocyte lineage commitment. *Blood*, **110**, 3871–3880.
78. Starck,J., Cohet,N., Gonnet,C., Sarrazin,S., Doubeikovskaia,Z., Doubeikovski,A., Verger,A., Duterque-Coquillaud,M. and Morle,F. (2003) Functional cross-antagonism between transcription factors FLI-1 and EKLF. *Mol. Cell. Biol.*, **23**, 1390–1402.
79. Tallack,M.R. and Perkins,A.C. (2010) Megakaryocyte-erythroid lineage promiscuity in EKLF null mouse blood. *Haematologica*, **95**, 144–147.
80. Starck,J., Weiss-Gayet,M., Gonnet,C., Guyot,B., Vicat,J.M. and Morle,F. (2010) Inducible Fli-1 gene deletion in adult mice modifies several myeloid lineage commitment decisions and accelerates proliferation arrest and terminal erythrocytic differentiation. *Blood*, **116**, 4795–4805.
81. Sim,K.G., Zang,Z., Yang,C.M., Bonventre,J.V. and Hsu,S.I. (2004) TRIP-Br links E2F to novel functions in the regulation of cyclin E expression during cell cycle progression and in the maintenance of genomic stability. *Cell Cycle*, **3**, 1296–1304.
82. Darwish,H., Cho,J.M., Loignon,M. and Alaoui-Jamali,M.A. (2007) Overexpression of SERTAD3, a putative oncogene located within the 19q13 amplicon, induces E2F activity and promotes tumor growth. *Oncogene*, **26**, 4319–4328.
83. Humbert,P.O., Rogers,C., Ganiatsas,S., Landsberg,R.L., Trimarchi,J.M., Dandapani,S., Brugnara,C., Erdman,S., Schrenzel,M., Bronson,R.T. *et al.* (2000) E2F4 is essential for normal erythrocyte maturation and neonatal viability. *Mol. Cell*, **6**, 281–291.
84. Dirlam,A., Spike,B.T. and Macleod,K.F. (2007) Deregulated E2f-2 underlies cell cycle and maturation defects in retinoblastoma null erythroblasts. *Mol. Cell. Biol.*, **27**, 8713–8728.
85. Wu,M.J., Wu,W.C., Chang,H.W., Lai,Y.T., Lin,C.H., Yu,W.C. and Chang,V.H. (2015) KLF10 affects pancreatic function via the SEI-1/p21Cip1 pathway. *Int. J. Biochem. Cell Biol.*, **60**, 53–59.
86. Song,C.Z., Gavriilidis,G., Asano,H. and Stamatoyannopoulos,G. (2005) Functional study of transcription factor KLF11 by targeted gene inactivation. *Blood Cells Mol. Dis.*, **34**, 53–59.
87. Mahabeleshwar,G.H., Kawanami,D., Sharma,N., Takami,Y., Zhou,G., Shi,H., Nayak,L., Jeyaraj,D., Grealy,R., White,M. *et al.* (2011) The myeloid transcription factor KLF2 regulates the host response to polymicrobial infection and endotoxic shock. *Immunity*, **34**, 715–728.
88. Alder,J.K., Georgantas,R.W. 3rd, Hildreth,R.L., Kaplan,I.M., Morisot,S., Yu,X., McDevitt,M. and Civin,C.I. (2008) Kruppel-like factor 4 is essential for inflammatory monocyte differentiation in vivo. *J. Immunol.*, **180**, 5645–5652.
89. Perkins,A.C., Yang,H., Crossley,P.M., Fujiwara,Y. and Orkin,S.H. (1997) Deficiency of the CACC-element binding protein, BKLF, leads to a progressive myeloproliferative disease and impaired expression of SHP-1. *Blood*, **90**, 2560–2560.
90. Bruce,S.J., Gardiner,B.B., Burke,L.J., Gongora,M.M., Grimmond,S.M. and Perkins,A.C. (2007) Dynamic transcription programs during ES cell differentiation towards mesoderm in serum versus serum-freeBMP4 culture. *BMC Genomics*, **8**, 365.
91. McConnell,B.B., Ghaleb,A.M., Nandan,M.O. and Yang,V.W. (2007) The diverse functions of Kruppel-like factors 4 and 5 in epithelial biology and pathobiology. *Bioessays*, **29**, 549–557.
92. Flandez,M., Guilmeau,S., Blache,P. and Augenlicht,L.H. (2008) KLF4 regulation in intestinal epithelial cell maturation. *Exp. Cell Res.*, **314**, 3712–3723.
93. Segre,J.A., Bauer,C. and Fuchs,E. (1999) Klf4 is a transcription factor required for establishing the barrier function of the skin. *Nat. Genet.*, **22**, 356–360.
94. Patel,S., Xi,Z.F., Seo,E.Y., McGaughey,D. and Segre,J.A. (2006) Klf4 and corticosteroids activate an overlapping set of transcriptional targets to accelerate in utero epidermal barrier acquisition. *Proc. Natl. Acad. Sci. U.S.A.*, **103**, 18668–18673.
95. Benzécri,J.P. (1982) Construction d'une classification ascendante hiérarchique par la recherche en chaîne des voisins réciproques. *Les Cahiers L'Analyse Donnees*, **7**, 209–218.
96. Juan,J. (1982) Programme de classification hiérarchique par l'algorithme de la recherche en chaîne des voisins réciproques. *Les Cahiers L'Analyse Donnees*, **7**, 219–225.